

1 **Title**

2 Going beyond clinical routine in SARS-CoV-2 antibody testing - A multiplex corona virus
3 antibody test for the evaluation of cross-reactivity to endemic coronavirus antigens
4

5 **Authors**

6 Matthias Becker^{1,#}, Monika Strengert^{2,3,#}, Daniel Junker¹, Tobias Kerrinnes⁴, Philipp D. Kaiser¹,
7 Bjoern Traenkle^{1,16}, Heiko Dinter^{1,16}, Julia Häring¹, Anne Zeck¹, Frank Weise¹, Andreas
8 Peter^{5,21,22}, Sebastian Hörber^{5,21,22}, Simon Fink¹, Felix Ruoff¹, Tamam Bakchoul⁹, Armin
9 Baillot¹⁰, Stefan Lohse¹¹, Markus Cornberg¹², Thomas Illig¹³, Jens Gottlieb¹⁴, Sigrun Smola¹¹,
10 André Karch¹⁷, Klaus Berger¹⁷, Hans-Georg Rammensee^{6,7,8}, Katja Schenke-Layland^{1,8,18,19},
11 Annika Nelde^{6,8,20}, Melanie Märklin^{8,20}, Jonas S. Heitmann^{8,20}, Juliane S. Walz^{6,8,15,20}, Markus
12 Templin¹, Thomas O. Joos¹, Ulrich Rothbauer^{1,16,#}, Gérard Krause^{2,3}, Nicole Schneiderhan-
13 Marra^{1,*}
14

15 **Affiliations**

16 ¹ NMI Natural and Medical Sciences Institute at the University of Tuebingen, Germany

17 ² Department of Epidemiology, Helmholtz Centre for Infection Research, Braunschweig,
18 Germany

19 ³ TWINCORE GmbH, Centre for Experimental and Clinical Infection Research, a joint venture
20 of the Hannover Medical School and the Helmholtz Centre for Infection Research, Hannover,
21 Germany

22 ⁴ Helmholtz-Institute for RNA-based Infection Research (HIRI), Würzburg, Germany

23 ⁵ Institute for Clinical Chemistry and Pathobiochemistry, Department for Diagnostic Laboratory
24 Medicine, University Hospital Tuebingen, Tuebingen, Germany

25 ⁶ Institute for Cell Biology, Department of Immunology, University of Tuebingen, Tuebingen,
26 Germany

27 ⁷ German Cancer Consortium (DKTK) and German Cancer Research Center (DKFZ), partner

28 **NOTE-** This preprint reports new research that has not been certified by peer review and should not be used to guide clinical practice.
site Tuebingen, Tuebingen, Germany.

29 ⁸ Cluster of Excellence iFIT (EXC2180) “Image-Guided and Functionally Instructed Tumor
30 Therapies”, University of Tuebingen, Tuebingen, Germany

31 ⁹ Institute for Clinical and Experimental Transfusion Medicine, University Hospital Tuebingen,
32 Tuebingen, Germany

33 ¹⁰ Niedersächsisches Landesgesundheitsamt, Department of Virology/Serology, Hannover,
34 Germany

35 ¹¹ Institute of Virology, Saarland University Medical Center, Homburg/Saar, Germany

36 ¹² Department of Gastroenterology, Hepatology, Endocrinology, Hannover Medical School,
37 Hannover, Germany; Centre for Individualized Infection Medicine (CiiM), Hannover, Germany

38 ¹³ Hannover Unified Biobank (HUB), Hannover Medical School, Hannover, Germany

39 ¹⁴ Clinic for Pneumonology, Hannover Medical School, Hannover, Germany

40 ¹⁵ Department of Hematology, Oncology, Clinical Immunology and Rheumatology, University
41 Hospital Tuebingen, Tuebingen, Germany

42 ¹⁶ Pharmaceutical Biotechnology, University of Tuebingen, Germany

43 ¹⁷ Institute of Epidemiology and Social Medicine, University of Münster, Münster, Germany

44 ¹⁸ Department of Women’s Health, Research Institute for Womens’s Health, Eberhard-Karls-
45 University, Tuebingen, Germany

46 ¹⁹ Department of Medicine/Cardiology, Cardiovascular Research Laboratories, David Geffen
47 School of Medicine at UCLA, Los Angeles, CA, USA

48 ²⁰ Clinical Collaboration Unit Translational Immunology, German Cancer Consortium (DKTK),
49 Department of Internal Medicine, University Hospital Tuebingen, Tuebingen, Germany

50 ²¹ Institute for Diabetes Research and Metabolic Diseases of the Helmholtz Center Munich at
51 the University of Tuebingen, Tuebingen, Germany

52 ²² German Center for Diabetes Research (DZD), München-Neuherberg, Germany

53 # These authors contributed equally to this work.

54

55

56

57 * Corresponding author:
58 Dr. Nicole Schneiderhan-Marra
59 Markwiesenstrasse 55, 72770 Reutlingen, Germany
60 Phone: 0049 7121 51530 815
61 Fax: 0049 7121 51530 16
62 E-Mail: Nicole.Schneiderhan@nmi.de

63 **Abstract**

64 Given the importance of the humoral immune response to SARS-CoV-2 as a global benchmark
65 for immunity, a detailed analysis is needed to monitor seroconversion in the general population,
66 understand manifestation and progression of COVID-19 disease, and ultimately predict the
67 outcome of vaccine development. In contrast to currently available serological assays, which
68 are only able to resolve the SARS-CoV-2 antibody response on an individual antigen level, we
69 developed a multiplex immunoassay, for which we included spike and nucleocapsid proteins
70 of SARS-CoV-2 and the endemic human coronaviruses (NL63, OC43, 229E, HKU1) in an
71 expanded antigen panel. Compared to three commercial *in vitro* diagnostic tests, our
72 MULTICOV-AB assay achieved the highest sensitivity and specificity when analyzing a well-
73 characterized sample set of SARS-CoV-2 infected and uninfected individuals. Simultaneously,
74 high IgG responses against endemic coronaviruses became apparent throughout all samples,
75 but no consistent cross-reactive IgG response patterns could be defined. In summary, we have
76 established and validated, a robust, high-content-enabled, and antigen-saving multiplex assay
77 MULTICOV-AB, which is highly suited to monitor vaccination studies and will facilitate
78 epidemiologic screenings for the humoral immunity toward pandemic as well as endemic
79 coronaviruses.

80

81 **Introduction**

82 Given the importance of the humoral immune response to SARS-CoV-2 as a global benchmark
83 for immunity, a detailed analysis is needed to (i) monitor seroconversion in the general
84 population^{1,2}, (ii) understand manifestation and progression of the disease^{3,4}, and (iii) predict
85 the outcome of vaccine development^{5,6}. Currently available serological assays utilize single
86 analyte technologies such as ELISA to measure antibodies against SARS-CoV-2 antigens
87 including spike (S) or nucleocapsid (N) protein^{1,6-8}. To measure individual antibody (IgG and
88 IgA) responses against SARS-CoV-2 and the endemic human coronaviruses (hCoVs) NL63,
89 229E, OC43, and HKU1, we developed a multiplexed immunoassay (MultiCoV-Ab), for which
90 we included S and N proteins of these coronaviruses in an expanded antigen panel. Compared
91 to commercial *in vitro* diagnostic (IVD) tests our MultiCoV-Ab assay achieved the highest
92 sensitivity and specificity when analyzing 310 SARS-CoV-2 infected and 866 uninfected
93 individuals. Simultaneously we see high IgG responses against hCoVs throughout all samples,
94 whereas no consistent cross reactive IgG response patterns can be defined. In summary, our
95 MultiCoV-Ab assay is highly suited to monitor vaccination studies and will facilitate
96 epidemiologic screenings for the humoral immunity toward pandemic as well as endemic
97 coronaviruses.

98 Results

99 To investigate the antibody response of SARS-CoV-2-infected individuals, we developed and
100 established a high-throughput and automatable bead-based multiplex assay, termed
101 MultiCoV-Ab. We expressed and immobilized six different SARS-CoV-2-specific antigens on
102 Luminex MAGPLEX beads with distinct color codes, specifically the trimeric full-length Spike
103 protein (Spike Trimer), receptor binding domain (RBD), S1 domain (S1), S2 domain (S2), full-
104 length nucleocapsid (N) and the N-terminal domain of nucleocapsid (N-NTD) (**Extended Data**
105 **Fig. 1**). Immunoglobulins from serum and plasma samples were detected using phycoerythrin-
106 labelled anti-human IgG or IgA antibodies. Data on quality control and assay performance is
107 provided in **Extended Data Fig. 2** and **Extended Data Table 1**.

108 As key antigens for the classification of SARS-CoV-2-induced seroconversion, we used Spike
109 Trimer and RBD previously described by Amanat *et. al*², and initially screened a set of 205
110 SARS-CoV-2-infected and 72 uninfected individuals with the MultiCoV-Ab assay. Using a
111 combined cut-off of both antigens, we identified all uninfected samples as negative (**Fig. 1a**).
112 Of the 205 infected samples, the MultiCoV-Ab assay identified 24 (11.7%) as IgG antibody-
113 negative. This finding is supported by three other commercially available IVD tests (Roche⁹,
114 Siemens Healthineers¹⁰, Euroimmun¹¹) widely used in clinical routine SARS-CoV-2 antibody
115 testing. However, the IVD tests missed additional 8 (Roche), 11 (Siemens Healthineers) and
116 9 (Euroimmun) samples of SARS-CoV-2-infected individuals. Furthermore, the Euroimmun
117 test classified 8 additional samples as “borderline” (**Fig. 1b**, **Extended Fig. 3a-c**). In
118 accordance with our MultiCoV-Ab assay, no samples were classified as false positives by the
119 Roche and Siemens tests, whereas one sample was classified as false positive and one as
120 “borderline” by the Euroimmun test.

121 When testing for IgA antibodies in samples of SARS-CoV-2-infected individuals, our MultiCoV-
122 Ab assay classified 47 (22.9 %) as IgA-negative, whereas the Euroimmun test classified 32
123 (15.6 %) as IgA-negative, and 16 (7.8 %) as borderline (**Fig. 1b** and **Extended Data Fig. 3d**).
124 For the uninfected samples, the Euroimmun test identified 7 (9.7 %) as false positives and 3

125 (4.2 %) as “borderline”, whereas no samples were classified as false positives by the MultiCoV-
126 Ab assay.

127 Next, we used an extended sample set with 310 SARS-CoV-2-infected and 866 uninfected
128 donors for clinical validation of MultiCoV-Ab assay. A simplified overview of this set is shown
129 in **Fig. 2a**; a complete breakdown is displayed in **Extended Data Table 2**. A direct comparison
130 revealed that Spike Trimer and RBD were the best predictors of SARS-CoV-2 infection. Signal
131 cut-offs were defined for both, IgG and IgA detection, based on ROC analysis with focus on
132 maximum specificity. Additionally, we defined a cut-off for overall IgG and IgA positivity for
133 which both individual cut-offs for Spike Trimer and RBD had to be met (**Fig. 2b**). As shown
134 above, cut-offs based on IgG were shown to be more sensitive and specific than those based
135 on IgA. With the IgG overall cut-off, we reached a specificity of 100 % (**Fig. 2c**), which would
136 not have been possible for either of the antigens individually, while still retaining acceptable
137 sensitivity. To identify samples with an early immune response, we simultaneously measured
138 IgA response. With the MultiCoV-Ab assay, we identified eight IgA-positive samples that
139 showed no IgG response (**Fig. 2d**). Two of these were uninfected and falsely classified as
140 positive. For four of the remaining six infected samples, details regarding the time between the
141 onset of symptoms and sample drawing were available (2, 6, 7, and 15 days). We hypothesized
142 that IgA in these samples can be used to measure an early onset of antibody response. Thus,
143 we classified samples with strong IgA positivity - signal to cut-off (S/CO) > 2 for Spike Trimer
144 and RBD - as “positive”, irrespective of their detected IgG response. With this
145 combined IgG + IgA classification, we reached an optimal sensitivity of 90 % while retaining a
146 specificity of 100 %.

147 Further analyzing the Ig response towards both subdomains of the spike, S1 and S2, we
148 achieved no additional sensitivity for the classifier (**Fig. 2e**). Interestingly, RBD, as a part of
149 S1, showed much fewer uninfected samples with increased IgG response compared to S1.
150 For S2 even more uninfected samples had increased signals, pointing to potential cross-
151 reactivity in this domain of the spike protein (**Fig. 2e**). We further complemented our assay
152 with the N and N-NTD proteins. Although these antigens were successfully used in single-

153 analyte assays¹², we observed a high cross reactivity in uninfected samples for both (**Fig. 2f**).
154 Across the entire data set, only one sample showed a distinct immune response to N and N-
155 NTD, but not to all spike derived antigens.

156 Longitudinal samples from five hospitalized patients were subjected to a small-scale time
157 course analysis of IgG and IgA immune responses (**Fig. 3a**). Levels of both Ig classes strongly
158 increased within the first ten days after the onset of symptoms. While IgG levels appeared
159 constant over roughly two months, IgA levels started to decline between day 10 and 20 after
160 the onset of symptoms where samples were available. These effects were consistent for the
161 majority of SARS-CoV-2 antigens. Furthermore, we found that patients' hospitalization, as a
162 measure of disease severity (**Fig. 3b**), seemed to correlate with an increased humoral immune
163 response, especially in IgA. Furthermore, there is indication for a trend for increasing age as
164 well (**Fig. 3c**). However, it should be considered that patients of higher age also had a higher
165 rate of hospitalization in our study population.

166 In order to explore cross-reactivity of hCoVs with SARS-CoV-2, we included S1, N, and N-NTD
167 antigens from human α - (NL63 and 229E) and β -hCoVs (OC43 and HKU1) in our MultiCoV-
168 Ab panel (**Extended Data Fig. 1**). The immune response towards all hCoV antigens was more
169 dependent on coronavirus clade than on N or S1 antigen. However, within the clades of α -
170 hCoVs and β -hCoVs, types of antigens were more dominant than the virus subtype, as
171 demonstrated by rank correlation analysis and hierarchical clustering. Interestingly, IgG
172 response against α -hCoVs clustered more closely to SARS-CoV-2 than to β -hCoVs (**Fig. 4a**,
173 **Extended Data Fig. 4a**). Overall, we identified a considerable immune response to hCoV
174 antigens throughout the whole sample set with no notable differences between samples from
175 SARS-CoV-2-infected and uninfected donors in IgG or IgA for S1 (**Fig. 4b**), N (**Fig. 4c**), or N-
176 NTD (**Extended Data Fig. 4b**).

177 We therefore used the IgG signal relative to the average response per antigen for further
178 analyses, which allowed comparison among all hCoV antigens on one scale. For those
179 uninfected samples, which showed an IgG cross reactivity towards Spike Trimer (Spike Trimer
180 false positives), we observed partially increased responses towards hCoV antigens. Those

181 samples, which did not show an immune response after SARS-CoV-2 infection (false
182 negatives, as determined by MultiCoV-Ab assay, combined IgG + IgA) were closer to the
183 baseline (**Fig. 4d-e, Extended Data Fig. 4c**). This indicates that cross-reactivity with hCoVs
184 causes some of the observed SARS-CoV-2 immune response in samples taken from
185 individuals not exposed to SARS-CoV-2.

186 To investigate the correlation of hCoV and SARS-CoV-2 immune response further, we grouped
187 samples into high and low responders for α -hCoVs and β -hCoVs. High responders had relative
188 IgG signals > 0 for N and S1 antigens of both hCoV subtypes within the clade, while low-
189 responders had < 0 , respectively. Samples with SARS-CoV-2 immune response (as
190 determined by MultiCoV-Ab assay, combined IgG + IgA classification) were significantly
191 overrepresented within the group of α -hCoV high responders ($p = 3.78e-03$, Fisher's exact
192 test, two sided), while being significantly underrepresented within the group of α -hCoV and β -
193 hCoV low responders ($p = 1.14e-03$ and $p = 1.56e-02$, respectively, Fisher's exact test, two
194 sided) (**Fig. 4f**). These results showed that while there were no discernible global effects for
195 single antigens, there is a correlation between the SARS-CoV-2 immune response with high
196 hCoV responses, especially towards α -hCoVs.

197 **Discussion**

198 We demonstrated that our MultiCoV-Ab, a novel multiplex assay, is highly suitable to classify
199 seroconversion in SARS-CoV-2-infected individuals. With a combined cut-off using SARS-
200 CoV-2 trimeric full-length spike protein and RBD, we were able to eliminate false positive
201 responses and achieved a sensitivity of 90% with a specificity of 100% for 310 samples from
202 SARS-CoV-2-infected and for 866 samples from uninfected individuals. We found that
203 detection of IgG more accurately reflected infection compared to IgA, although both were highly
204 specific. However, by simultaneously monitoring IgA, we additionally were able to detect an
205 early immune response in some patients. The MultiCoV-Ab approach allows the easy addition
206 of SARS-CoV-2-specific antigens, here six in total, which provides an additional level of
207 confidence in patient classification. Thus, for example, we noticed that the spike S1 domain
208 showed fewer false positive responses compared to the S2 domain. Interestingly, Ng *et al.*¹³
209 reported reactivity towards SARS-CoV-2 S2 from sera of patients with recent seasonal hCoV
210 infection. These sera prevented infection with SARS-CoV-2 pseudotypes in a neutralization
211 assay. Additionally, we found that spike non-responders also did not show a response to
212 nucleocapsid, which has been described as strongest inducer of antibody responses^{12,14}; and
213 not vice versa.

214 In our comparison to commercially available IVD tests, we classified fewer samples as false
215 negative using our MultiCoV-Ab assay. For 10% of all infected samples, we could not detect a
216 SARS-CoV-2 specific immune response, which is in line with previous findings^{3,15,16}. Those
217 non-responders may be able to limit viral replication by innate immune mechanisms or cellular
218 immunity is dominant in mediating viral clearance^{17,18}.

219 Expanding our MultiCoV-Ab assay to the endemic hCoVs NL63, 229E, OC43, and HKU1
220 revealed a clear IgG immune response for all tested samples. Furthermore, we did not observe
221 a difference for the samples from proven hCoV-infected individuals, compared to other
222 samples. Due to the general lack of availability of samples from hCoV-naïve individuals, it was
223 difficult to analyze hCoV-mediated cross-reactivity. Nevertheless, our multiplexed readout
224 indicates a correlation between the SARS-CoV-2 immune response and high hCoV responses.

225 Currently, we are identifying population groups which were highly exposed and showed
226 different susceptibility to SARS-CoV-2 infection, e.g. the “Ischgl-study group” (unpublished
227 data)¹⁹, in order to elucidate potential cross protection derived from immune responses towards
228 endemic hCoVs in more detail. Alternatively, studies analyzing hCoV signatures in samples
229 from individuals before and after SARS-CoV-2 infection using the MultiCoV-Ab assay would
230 help to get insight into a potential cross protection.

231 A multiplex setup such as MultiCoV-Ab assay is especially suited to vaccination studies, since
232 the flexibility and broad antigen coverage allows to efficiently map vaccine immune responses
233 to an immunoglobulin isotype and subtype level for the target pathogen and related species ²⁰.
234 Interestingly, previous SARS-CoV-1 vaccine studies clearly indicated that a detailed
235 characterization of vaccine-induced antibody responses is mandatory for efficient coronavirus
236 vaccine development^{21,22}.

237 In summary, we have established and validated the MultiCoV-Ab assay, a robust, high-
238 content-enabled, and antigen-saving multiplex assay. This assay is suitable for comprehensive
239 characterization of SARS-CoV-2 infection on the humoral immune response and for
240 epidemiological screenings to accurately measure SARS-CoV-2 seroprevalence in large
241 cohort studies. It further provides the unique opportunity to assess and correlate immunity for
242 both endemic and pathogenic coronaviruses. Finally, the multiplex nature of the MultiCoV-Ab
243 assay can deliver urgently needed data on the outcome of SARS-CoV-2 vaccination.

244 **Supplementary - Materials and Methods**

245 **Generation of expression constructs for production of viral antigens**

246 The cDNAs encoding the full-length nucleocapsid proteins of SARS-CoV-2, hCoV-OC43,
247 hCoV-NL63, hCoV-229E, and hCoV-HKU1 (GenBank accession numbers QHD43423.2;
248 YP_009555245.1; YP_003771.1; NP_073556.1; YP_173242.1) were produced with an N-
249 terminal hexahistidine (His₆)-tag by DNA synthesis (ThermoFisher Scientific). The cDNAs were
250 cloned by standard techniques into NdeI/HindIII sites of the bacterial expression vector
251 pRSET2b (ThermoFisher Scientific). To generate N-terminal domains (NTDs) of the respective
252 nucleocapsid proteins (SARS-CoV-2 NTD aa 1-189; hCoV-OC43 NTD aa 1-204; hCoV-NL63
253 NTD aa 1 - 154; hCoV-229E NTD aa 1-156; hCoV-HKU1 NTD aa 1- 203), a stop codon located
254 N-terminally to the Serine-Arginine (SR)-rich linker site²³ was introduced via PCR mutagenesis
255 of the nucleocapsid encoding plasmids using the forward primer pRSET2b down-for 5' - GGT
256 AAG CTT GAT CCG GCT GCT AA - 3' and respective reverse primers: SARS-CoV2_NTD-rev
257 5' - GGG AAG CTT ACT CAG CAT AGA AGC CCT TTG G - 3', OC43_NTD-rev 5' - GGG AAG
258 CTT ATT CGA TAT AAT AGC CCT GCG G - 3', NL63_NTD-rev 5' - GGG AAG CTT ATT CAA
259 CAA CGC TCA GTT CCG - 3', 229E_NTD-rev 5' - GGG AAG CTT ATT CAA CAA CGG TAA
260 CAC CAT TC - 3' and HKU1_NTD-rev 5' - GGG AAG CTT ATT CCA CAT AGT AGC CCT
261 GAG GC - 3'.

262 The pCAGGS plasmids encoding the stabilized trimeric Spike protein and the receptor binding
263 domain (RBD) of SARS-CoV-2 were kindly provided by F. Krammer².

264 The cDNA encoding the S1 domain (aa 1 - 681) of the SARS-CoV-2 Spike protein was
265 obtained by PCR amplification using the forward primer S1_CoV2-for 5'- CTT CTG GCG TGT
266 GAC CGG - 3' and reverse primer S1_CoV2-rev 5' - GTT GCG GCC GCT TAG TGG TGG
267 TGG TGG TGG TGG GGG CTG TTT GTC TGT GTC TG - 3' and the full length SARS-CoV-
268 2 SPIKE cDNA as template and cloned into the XbaI/NotI-digested backbone of the pCAGGS
269 vector, thereby adding a C-terminal His₆-Tag.

270 The cDNAs encoding the S1 domains of hCoV-OC43 (aa 1 -760), hCoV-NL63 (aa 1 - 744),
271 hCoV-229E (aa 1 - 561) and hCoV-HKU1 (aa 1 - 755) (GenBank accession numbers

272 AVR40344.1; APF29071.1; YP_003771.1; APT69883.1; AGW27881.1) were produced by
273 DNA synthesis (ThermoFisher Scientific), digested using XbaI/NotI and ligated into the
274 pCAGGS vector. All expression constructs were verified by sequence analysis.

275

276 **Protein expression and purification**

277 For expression of the viral nucleocapsid proteins (full-length nucleocapsid and N-NTDs), the
278 respective expression constructs were used to transform *E.coli* BL21 (DE3) cells. Protein
279 expression was induced in 1 L TB medium at an optical density (OD₆₀₀) of 2.5 - 3 by addition
280 of 0.2 mM isopropyl-β-D-thiogalactopyranoside (IPTG) for 16 h at 20 °C. Cells were harvested
281 by centrifugation (10 min at 6,000 x g) and the pellets were suspended in binding buffer
282 (1x PBS, ad 0.5 M NaCl, 50 mM imidazole, 2 mM phenylmethylsulfonyl fluoride, 2 mM MgCl₂,
283 150 µg/mL lysozyme (Merck) and 625 µg/mL DNaseI (Applichem)). Cell suspensions were
284 sonified for 15 min (Bandelin Sonopuls HD70 - power MS72/D, cycle 50%) on ice, incubated
285 for 1 h at 4 °C in a rotary shaker followed by a second sonification step for 15 min. After
286 centrifugation (30 min at 20,000 x g), urea was added to a final concentration of 6 M to the
287 soluble protein extract. The extract was filtered through a 0.45 µm filter and loaded on a pre-
288 equilibrated 1-mL HisTrap^{FF} column (GE Healthcare). The bound His-tagged nucleocapsid
289 proteins were eluted by a linear gradient (30 mL) ranging from 50 to 500 mM imidazole in
290 elution buffer (1x PBS, pH 7.4, 0.5 M NaCl, 6 M urea). Elution fractions (0.5 mL) containing the
291 His-tagged nucleocapsid proteins were pooled and dialyzed (D-Tube Dialyzer Mega, Novagen)
292 against PBS.

293 The viral S1-domains, SARS-CoV-2 RBD, and the stabilized trimeric SARS-CoV-2 Spike
294 protein were expressed in Expi293 cells following the protocol as described in Stadlbauer *et*
295 *al.*⁸.

296 All purified proteins were analyzed via standard SDS-PAGE followed by staining with
297 InstantBlue Coomassie stain (Expedeon) and immunoblotting using an anti-His antibody
298 (Penta-His Antibody, #34660, Qiagen) in combination with a donkey-anti-mouse antibody
299 labeled with AlexaFluor647 (Invitrogen) on a Typhoon Trio (GE-Healthcare, Freiburg,

300 Germany; excitation 633 nm, emission filter settings 670 nm BP 30) to confirm protein integrity.
301 To further confirm correct expression, integrity, and purity, proteins were analysed by mass
302 spectrometry. To control the production reproducibility of the antigens, potential aggregation
303 and melting temperatures of the proteins were investigated by nano differential scanning
304 fluorimetry (nanoDSF) using a Prometheus (Nanotemper, Munich, Germany).

305

306 **Commercial antigens**

307 Two commercial antigens were used to complement the in-house-produced antigen panel.
308 The S2 ectodomain of the SARS-CoV-2 spike protein (aa 686 – 1213) was purchased from
309 Sino Biological, Eschborn, Germany (cat # 40590, lot # LC14MC3007). A full-length
310 nucleocapsid protein of SARS-CoV-2 was purchased from Aalto Bioreagents, Dublin, Ireland
311 (cat # 6404-b, lot # 4629).

312

313 **Bead-based serological multiplex assay**

314 All antigens were covalently immobilized on spectrally distinct populations of carboxylated
315 paramagnetic beads (MagPlex Microspheres, Luminex Corporation, Austin, TX) using 1-ethyl-
316 3-(3-dimethylaminopropyl)carbodiimide (EDC)/ sulfo-N-hydroxysuccinimide (sNHS) chemistry.
317 For immobilization, a magnetic particle processor (KingFisher 96, Thermo Scientific, Schwerte,
318 Germany) was used.

319 Bead stocks were vortexed thoroughly and sonicated for 15 seconds. Subsequently, 83 μL of
320 0.065% (v/v) Triton X-100 and 1 mL of bead stock containing 12.5×10^7 beads of one single
321 bead population were pipetted into each well. The beads were then washed twice with 500 μL
322 of activation buffer (100 mM Na_2HPO_4 , pH 6.2, 0.005% (v/v) Triton X-100) and beads were
323 activated for 20 min in 300 μL of activation mix containing 5 mg/mL EDC and 5 mg/mL sNHS
324 in activation buffer. Following activation, the beads were washed twice with 500 μL of coupling
325 buffer (500 mM MES, pH 5.0, 0.005% (v/v) Triton X-100) and the antigens were added to the
326 activated beads and incubated for 2 h at 21 °C to immobilize the antigens on the surface.

327 Antigen-coupled beads were washed twice with 800 μ L of wash buffer (1x PBS, 0.005 % (v/v)
328 Triton X-100) and were finally resuspended in 1,000 μ L of storage buffer (1x PBS, 1 % (w/v)
329 BSA, 0.05% (v/v) ProClin). The beads were stored at 4°C until further use.
330 To detect human IgG and IgA responses against SARS-CoV-2 and the endemic human
331 coronaviruses (hCoV-NL63, hCoV-229E, hCoV-OC43 and hCoV-HKU1), the purified trimeric
332 Spike protein (S), S1-domain, S2-domain (Sino Biological GmbH, Europe), RBD, nucleocapsid
333 (N) and the N-terminal domain of nucleocapsid (N-NTD) of SARS-CoV-2 as well as the S1-
334 domain, N, and N-NTD of the endemic hCoVs were immobilized on different bead populations
335 as described above. The individual bead populations were combined into a bead mix. A bead-
336 based multiplex assay was performed. Briefly, samples were incubated at a 1:400 dilution for
337 2 hours at 21 °C. Unbound antibodies were removed and the beads were washed three times
338 with 100 μ L of wash buffer (1x PBS, 0.05% (v/v) Tween20) per well using a microplate washer
339 (Biotek 405TS, Biotek Instruments GmbH). Bound antibodies were detected with R-
340 phycoerythrin labeled goat-anti-human IgG or IgA antibodies (incubation for 45 min at 21°C).
341 Measurements were performed using a Luminex FLEXMAP 3D instrument and the Luminex
342 xPONENT Software 4.3 (settings: sample size: 80 μ L, 50 events, Gate: 7,500 – 15,000,
343 Reporter Gain: Standard PMT).

344

345 **Data analysis**

346 Data analysis and visualization was performed with R Studio (Version 1.2.5001, using R
347 version 3.6.1) using the Median Fluorescent Intensity (MFI). Statistical analysis was performed
348 using R package “stats” from the base repository. Mann-Whitney U test was used to determine
349 difference between signal distributions from different sample groups. Spearman’s ρ coefficient
350 was calculated in order to correlate antigens by response from the entire sample set, followed
351 by hierarchical clustering to group antigens. Fishers’ exact test was used to calculate
352 significance of overlap between sample groups.

353

354

355 **Quality control**

356 In order to test the repeatability of the MultiCoV-Ab assay three quality control samples (QCs)
357 were processed in duplicate on each test plate (n = 17) during the sample screening and inter-
358 assay variance was assessed for each antigen in the multiplex. For intra-assay variance, 24
359 replicates for each of the three QC samples were analyzed on one plate. Achieved results are
360 presented in **Extended Data Table 1 and Extended Data Fig. 2**. A limit of detection (LOD)
361 for each antigen was determined by processing a blank in 24 replicates and LOD was set as
362 mean MFI + 3 standard deviations. Sample parallelism and comparability of paired serum and
363 plasma samples was assessed over eight dilution steps ranging from 1:100 to 1:12,800
364 (**Extended Data Fig. 2**). A set of samples derived from 205 SARS-CoV-2-infected and 72
365 uninfected individuals was tested repeatedly with two different kit batches. The samples
366 classification in both runs matched 100 %.

367

368 **Samples**

369 A total of 1176 sera and plasma samples were used for the MultiCoV-Ab assay development.
370 Ethical approval was granted from the Ethics Committee of Hannover Medical School
371 (#9122_BO_K2020). Only de-identified samples were used for the MultiCoV-Ab assay
372 development. All samples were pre-existing. Cohort age was 5-88 years; age was not known
373 for 161 samples.

374 310 samples were from COVID-19 patients or convalescents. Samples were classified as
375 SARS-CoV-2 infected, if a positive SARS-CoV-2 RT-PCR was reported and/ or if
376 hospitalization/ quarantine for COVID-19 was indicated as part of the samples metadata. ΔT
377 defined as time between PCR test or symptom onset and blood draw was 0-73 days (median=
378 38 d; n=258). ΔT was not provided for 52 samples. SARS-CoV-2 infected samples used in this
379 study were collected after ethical review (9001_BO_K, Hannover Medical School;
380 179/2020/BO2, University Hospital Tübingen; 85/20, Ärztekammer des Saarlandes).

381 866 control samples were from non-SARS-CoV-2 infected individuals and were classified as
382 non-infected as they were obtained prior to the emergence of SARS-CoV-2 in December 2019

383 or because they were taken from individuals who had not reported cold symptoms since the
384 beginning of 2020.

385 The majority of non-SARS-COV-2 infected samples was randomly selected and consistent of
386 prepandemic blood donors, commercially available (Central BioHub GmbH, Berlin, Germany
387 and BBI Solutions, Crumlin, UK) or bio-banked specimens. 365 samples were from the
388 Memory and Morbidity in Augsburg Elderly (MEMO) study (a subcohort of the MONICA S2
389 cohort (WHO 1988)) and were included based on available serological titers for HSV-1, HSV-
390 2, HHV-6 and EBV²⁴. 88 samples were obtained from transplanted patients with chronic
391 respiratory conditions.

392 Collection of non-SARS-CoV-2 infected control samples had been approved by several ethic
393 votes: 3232-2016 (Ethics Committee of Hannover Medical School); 62/20 (Ethics Committees
394 of the Medical Faculty of the Saarland University at the Saarland Ärztekammer); WUM
395 17.02.1997 (Joint ethics committee of the University of Muenster and the Westphalian
396 Chamber of Physicians),

397 Additional sample details can be found in Extended Data Table 2.

398

399 **Data availability**

400 Primary Data including raw MFI and sample annotation will be made available upon request.

401

402 **Code availability**

403 R Code for data analysis will be made available upon request.

404 **References**

- 405 1. Okba, N.M.A., et al. Severe Acute Respiratory Syndrome Coronavirus 2-Specific
406 Antibody Responses in Coronavirus Disease Patients. *Emerg Infect Dis* 26, 1478-1488
407 (2020).
- 408 2. Amanat, F., et al. A serological assay to detect SARS-CoV-2 seroconversion in humans.
409 *Nat Med* (2020).
- 410 3. Tan, W., et al. Viral Kinetics and Antibody Responses in Patients with COVID-19.
411 medRxiv, 2020.2003.2024.20042382 (2020).
- 412 4. Long, Q.X., et al. Antibody responses to SARS-CoV-2 in patients with COVID-19. *Nat*
413 *Med* 26, 845-848 (2020).
- 414 5. Amanat, F. & Krammer, F. SARS-CoV-2 Vaccines: Status Report. *Immunity* 52, 583-589
415 (2020).
- 416 6. Robbiani, D.F., et al. Convergent antibody responses to SARS-CoV-2 in convalescent
417 individuals. *Nature* (2020).
- 418 7. Lassaunière, R., et al. Evaluation of nine commercial SARS-CoV-2 immunoassays.
419 (medRxiv, 2020).
- 420 8. Stadlbauer, D., et al. SARS-CoV-2 Seroconversion in Humans: A Detailed Protocol for a
421 Serological Assay, Antigen Production, and Test Setup. *Curr Protoc Microbiol* 57, e100
422 (2020).
- 423 9. <https://diagnostics.roche.com/global/en/products/params/electsys-anti-sars-cov-2.html>.
- 424 10. [https://www.siemens-healthineers.com/de/laboratory-diagnostics/assays-by-diseases-](https://www.siemens-healthineers.com/de/laboratory-diagnostics/assays-by-diseases-conditions/infectious-disease-assays/cov2t-assay)
425 [conditions/infectious-disease-assays/cov2t-assay](https://www.siemens-healthineers.com/de/laboratory-diagnostics/assays-by-diseases-conditions/infectious-disease-assays/cov2t-assay).
- 426 11. <https://www.coronavirus-diagnostik.de/antikoerpertestsysteme-fuer-covid-19.html>.
- 427 12. Burbelo, P.D., et al. Detection of Nucleocapsid Antibody to SARS-CoV-2 is More
428 Sensitive than Antibody to Spike Protein in COVID-19 Patients. medRxiv (2020).
- 429 13. Ng, K., et al. Pre-existing and de novo humoral immunity to SARS-CoV-2 in humans.
430 bioRxiv, 2020.2005.2014.095414 (2020).

- 431 14. Sun, B., et al. Kinetics of SARS-CoV-2 specific IgM and IgG responses in COVID-19
432 patients. *Emerg Microbes Infect* 9, 940-948 (2020).
- 433 15. den Hartog, G., et al. SARS-CoV-2-specific antibody detection for sero-epidemiology: a
434 multiplex analysis approach accounting for accurate seroprevalence. *medRxiv*,
435 2020.2006.2018.20133660 (2020).
- 436 16. Wang, H., et al. SARS-CoV-2 proteome microarray for mapping COVID-19 antibody
437 interactions at amino acid resolution. *bioRxiv*, 2020.2003.2026.994756 (2020).
- 438 17. Nelde, A., et al. SARS-CoV-2 T-cell epitopes define heterologous and COVID-19-
439 induced T-cell recognition. (2020).
- 440 18. Liu, L., et al. Anti-spike IgG causes severe acute lung injury by skewing macrophage
441 responses during acute SARS-CoV infection. *JCI Insight* 4(2019).
- 442 19. [https://science.apa.at/rubrik/medizin_und_biotech/lschgl-](https://science.apa.at/rubrik/medizin_und_biotech/lschgl-Studie_42_4_Prozent_sind_Antikoerper-positiv/SCI_20200625_SCI39451352255218286)
443 [Studie_42_4_Prozent_sind_Antikoerper-](https://science.apa.at/rubrik/medizin_und_biotech/lschgl-Studie_42_4_Prozent_sind_Antikoerper-positiv/SCI_20200625_SCI39451352255218286)
444 [positiv/SCI_20200625_SCI39451352255218286](https://science.apa.at/rubrik/medizin_und_biotech/lschgl-Studie_42_4_Prozent_sind_Antikoerper-positiv/SCI_20200625_SCI39451352255218286).
- 445 20. Okba, N.M.A., et al. Particulate multivalent presentation of the receptor binding domain
446 induces protective immune responses against MERS-CoV. *Emerg Microbes Infect* 9,
447 1080-1091 (2020).
- 448 21. Yasui, F., et al. Prior immunization with severe acute respiratory syndrome (SARS)-
449 associated coronavirus (SARS-CoV) nucleocapsid protein causes severe pneumonia in
450 mice infected with SARS-CoV. *J Immunol* 181, 6337-6348 (2008).
- 451 22. Bolles, M., et al. A double-inactivated severe acute respiratory syndrome coronavirus
452 vaccine provides incomplete protection in mice and induces increased eosinophilic
453 proinflammatory pulmonary response upon challenge. *J Virol* 85, 12201-12215 (2011).
- 454 23. Kang, S., et al. Crystal structure of SARS-CoV-2 nucleocapsid protein RNA binding
455 domain reveals potential unique drug targeting sites. *Acta Pharm Sin B* (2020).
- 456 24. Zeeb, M., et al. Seropositivity for pathogens associated with chronic infections is a risk
457 factor for all-cause mortality in the elderly: findings from the Memory and Morbidity in
458 Augsburg Elderly (MEMO) Study. *GeroScience* (2020).

459 **Acknowledgements**

460 This work has received funding from the European Union's Horizon 2020 research and
461 innovation programme under grant agreement No 101003480 – CORESMA as well as from
462 the German Federal Ministry for Research and Education/the Helmholtz Association. We thank
463 Florian Krammer providing us with expression plasmids for the Spike Trimer and RBD. We
464 thank Shannon Layland for critical proofreading of the manuscript.

465

466 **Author Contributions**

467 M.B. designed and performed experiments and data analysis; M.S. designed experiments;
468 D.J., J.H., S.F., F.R., planned and performed experiments; A.Z. performed mass spectrometry
469 analysis; J.H. performed nanoDSF analyses; H.D., B.T., P.K., F.W., U.R. designed, cloned,
470 expressed and purified the antigens; S.H. and A.P. performed sample analysis; T.B., A.B.,
471 S.L., S.S., M.C., T.I., H-G.R., A.N., J.W., M.T., T.O.J. arranged sample and data collection;
472 M.T., T.O.J, G.K. supported the study planning; N.S-M. planned the assay development and
473 validation and designed experiments; M.B., M.S., U.R. and N.S-M. wrote the manuscript. All
474 authors reviewed the manuscript.

475

476 **Competing interests**

477 T.O.J is a scientific advisor for Luminex. N.S-M. was a speaker at Luminex user meetings in
478 the past. The Natural and Medical Sciences Institute at the University of Tuebingen is involved
479 in applied research projects as a fee for services with Luminex.

480 **Figure Legends**

481

482 **Fig. 1. | MultiCoV-Ab assay, a sensitive and specific tool to monitor SARS-CoV-2**
483 **antibody responses. a**, Control sera (blue, n = 72) and sera from individuals with PCR-
484 confirmed SARS-CoV-2 infection (red, n = 205) were screened in a multiplex bead-based
485 assay using Luminex technology (MultiCoV-Ab) to quantify IgG or IgA responses to various
486 antigens. Reactivity towards trimeric SARS-CoV-2 spike protein (Spike Trimer) or SARS-CoV-
487 2 receptor binding domain of spike (RBD) was found to be the best predictor of SARS-CoV-2
488 infection. Data are presented as Box-Whisker plots of sample median fluorescence intensity
489 (MFI) on a logarithmic scale. Outliers determined by 1.5 times IQR of log-transformed data are
490 depicted as circles. **b**, Sample set from **a**, was used to compare assay performance of the
491 MultiCoV-Ab assay using combined Spike Trimer and RBD antigens with commercially
492 available single analyte SARS-CoV-2 assays which detect total Ig (Elecsys Anti-SARS-CoV-2
493 (Roche); ADVIA Centaur SARS-CoV-2 Total (COV2T) (Siemens Healthineers)) or IgG (Anti-
494 SARS-CoV-2-ELISA - IgG (Euroimmun)) or IgA (Anti-SARS-CoV-2-ELISA - IgA (Euroimmun)).
495 SARS-CoV-2 infection status of samples is indicated as SARS-CoV-2 positive (PCR) or
496 negative. Antibody test results were classified as negative (blue), positive (red) or borderline
497 (grey) as per the manufacturer's definition. Only samples with divergent antibody test results
498 are shown.

499 **Fig. 2. | Combination of 2 Spike protein variants and isotype profiling by multiplex assay**
500 **increases accuracy to identify SARS-CoV-2 antibody positive individuals.**

501 **a**, An extended sample set of SARS-CoV-2-uninfected (n = 866) and SARS-CoV-2-infected
502 individuals (n = 310) was used to further validate our MultiCoV-Ab assay. Age, gender, SARS-
503 CoV-2 infection status and hospitalization status of study population are shown. NA:
504 information was not provided. **b**, MultiCoV-Ab assay sensitivity and specificity were calculated
505 for IgA or IgG based on a single analyte or a combined cut-off of Spike Trimer and RBD (IgG
506 or IgA overall). A cut-off combining IgG and IgA was calculated as well. **c-d**, Scatterplot
507 detailing MultiCoV-Ab assay cut-offs. Signal to cut-off (S/CO) values are displayed for Spike
508 Trimer against RBD on a logarithmic scale. For IgG (**c**), cut-offs are visualized by straight lines
509 and SARS-CoV-2-infected and uninfected samples are separated by color (black circles –
510 SARS-CoV-2-uninfected; red circles – SARS-CoV-2-infected). For IgA (**d**), cut-offs are
511 visualized as dashed lines and S/CO of 2 used for the combined cut-off is shown as straight
512 lines. SARS-CoV-2-infected samples are split into IgG-positives and -negatives by color as
513 indicated in the plot. **e-f**, Scatterplots display IgG response to additional SARS-CoV-2 antigens
514 contained in the MultiCoV-Ab panel: MFI for Spike subdomains S1 vs S2 (**e**), or Nucleocapsid
515 antigens N vs N-NTD (**f**), are displayed on logarithmic scale. SARS-CoV-2-uninfected samples
516 are distinguished from SARS-CoV-2-infected and MultiCoV-Ab classification into positives or
517 negatives as indicated by color.

518 **Fig. 3. | Multiplex-based seroprofiling allows in-depth characterization of SARS-CoV-2**
519 **antibody responses**

520 **a**, Kinetic of SARS-CoV-2 antigen-specific IgA and IgG responses is shown for indicated days
521 after symptom onset for six SARS-CoV-2-specific antigens for five different patients. **b-c**,
522 Samples of SARS-CoV-2-infected individuals were analysed to identify antigen- and isotype-
523 specific antibody responses based on hospitalization indicating disease severity (**b**,) or age
524 (**c**,). Data is presented as Box-Whisker plots of sample MFI on a logarithmic scale. Outliers
525 determined by 1.5 times IQR of log-transformed data are depicted as circles. p-value (Mann-
526 Whitney U test, two-sided) is displayed at the top of the boxes, indicating differences between
527 signal distribution for respective groups.

528 **Fig. 4. | Correlation of endemic and SARS CoV-2 antibody responses**

529 **a**, Correlation of IgG response for the entire sample set ($n = 1176$) is visualized as heatmap
530 based on Spearman's ρ coefficient; dendrogram on the right side displays antigens after
531 hierarchical clustering was performed. **b-c**, Immune responses (IgG and IgA) towards hCoV
532 S1 (**b**,) and N (**c**,) proteins are presented as Box-Whisker plots of sample MFI on a logarithmic
533 scale for SARS-CoV-2-infected (red, $n = 310$) and uninfected (blue, $n = 866$) individuals.
534 Outliers determined by 1.5 times IQR of log-transformed data are depicted as circles. **d-e**,
535 Relative levels of IgG-specific immune response towards hCoV S1 (**d**,) and N (**e**,) proteins are
536 presented as Box-Whisker plots / stripchart overlays of log-transformed and per-antigen
537 scaled and centred MFI for the sample subsets of Spike Trimer false positives (blue, $n = 17$)
538 and combined IgG + IgA false negatives (red, $n = 31$). **f**, From the entire study population,
539 groups of α - or β -hCoV high and low responders were built as indicated. High responder were
540 defined as samples with above average MFI values for S1 and N-specific IgGs of the
541 respective hCoV clade. Low responders were defined with below MFI values, correspondingly.
542 Responder groups (i) α -hCoV \uparrow , red, $n = 233$, (ii) β -hCoV \uparrow , green, $n = 254$, (iii) α -hCoV \downarrow , blue,
543 $n = 172$ (iv) β -hCoV \downarrow , purple, $n = 210$ are shown as Box-Whisker plots of log-transformed and
544 per-antigen scaled and centred MFI values across hCoV N and S1 antigens. Outliers
545 determined by 1.5 times IQR are depicted as circles. The over- or under-representation of
546 SARS-CoV-2 responders (SARS-CoV-2 +, $n = 279$, as determined by positive MultiCoV-Ab
547 classification) within the four sample groups is visualized in Venn diagrams, stochastic
548 significance was calculated using Fisher's exact test (two-sided).

549

550 **Extended Data Figure Legends**

551 **Extended Data Fig.1**

552 SDS-PAGE analysis of the recombinant viral antigens used in this study. To test for purity and
553 integrity 1 - 2 µg of indicated recombinant proteins were boiled in reducing SDS-sample buffer
554 and subjected to a gradient (4 - 20%) SDS-PAGE followed by coomassie staining. SARS-CoV-
555 2_Spike, SARS-CoV-2_RBD and the S1-domains of SARS-CoV-2, hCoV-NL63, hCoV-229E,
556 hCoV-OC43 and hCoV-HKU1 were produced in ExpiHEK™ cells. Nucleocapsid (N) and N-
557 terminal domain of nucleocapsid (N-NTD) of SARS-CoV-2, hCoV-NL63, hCoV-229E, hCoV-
558 OC43 and hCoV-HKU1 were produced in *E.coli*.

559

560 **Extended Data Fig.2**

561 **a**, Three quality control (QC) samples, as well as a sample of assay buffer (blank sample) were
562 processed in duplicates on every plate. Performance across 17 assay runs is depicted and
563 mean and %CVs are shown on the left side. For plate 14, a processing error lead to exclusion
564 of one blank sample from this evaluation. **b**, To assess parallelism of signals from different
565 samples, 6 unique serum samples were processed over a dilution series of 8 steps from 1:100
566 to 1:12,800. For 3 samples, paired plasma (EDTA and/or Heparin) were available and
567 processed together. For IgG and IgA detection of Spike Trimer and RBD, MFI are plotted
568 against sample dilution. Color indicates unique sample and shapes indicate sample type.

569

570 **Extended Data Fig.3**

571 **a-d**, Scatterplots of sample set with defined SARS-CoV-2 infection status (infected: red, n=205;
572 uninfected: black, n=72) to compare performance of the MultiCoV-Ab Spike Trimer vs indicated
573 antigens of commercial SARS-CoV-2 test kits. Signals are depicted as Signal to cut-off ratios
574 (S/CO) on a logarithmic scale. Lines indicate the respective cut-off values as defined by the
575 manufacturer to determine positive and negative test results.

576

577

578 **Extended Data Fig.4**

579 **a**, Correlation of IgA response for the entire sample set (n=1176) is visualized as heatmap
580 based on Spearman's ρ coefficient; dendrogram on the right side displays antigens after
581 hierarchical clustering was performed. **b**, Immune response (IgG and IgA) towards hCoV N-
582 NTD proteins are presented as Box-Whisker plots of sample MFI on a logarithmic scale for
583 SARS-CoV-2-infected (red, n=310) and uninfected (blue, n=866) individuals. Outliers
584 determined by 1.5 times IQR of log-transformed data are depicted as circles. **c**, Relative levels
585 of IgG-specific immune response towards hCoV N-NTD proteins are presented as Box-
586 Whisker plots / stripchart overlays of log-transformed and per-antigen scaled and centred MFI
587 for the sample subsets of Spike Trimer false positives (blue, n=17) and combined IgG + IgA
588 false negatives (red, n=31).

589

590 **Extended Data Table 1**

591 Intra- and inter-assay variance were determined by repeated measurement of QC samples
592 and blank sample as replicates on one plate and in duplicates over 17 plates, respectively.
593 Standard deviation relative to mean (%CV) is given for each antigen. A limit of detection (LOD)
594 was calculated from 24 blank sample replicates on the same plate as the mean MFI + 3 times
595 standard deviation.

596

597 **Extended Data Table 2**

598 Complete overview of study sample set. Samples are divided into columns by age groups and
599 gender. NA: Information was not available. Samples from SARS-CoV-2-infected donors are
600 further split up by hospitalization status. Age and gender of patients from which multiple
601 samples were available for time course analyses are indicated. SARS-CoV-2-uninfected
602 samples are further divided into samples drawn during the pandemic, which was defined as all
603 samples taken on 01.01.2020 or later, and pre-pandemic samples. 147 samples with previous
604 hCoV infection were included in the SARS-CoV-2-uninfected group. Detailed diagnosis of
605 hCoV subspecies is indicated where available. Other sample conditions for special groups of
606 uninfected samples are listed.

Figure 1

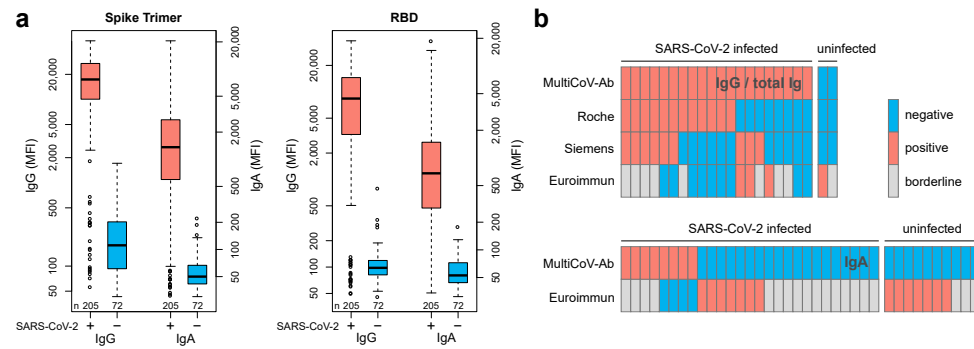


Figure 2

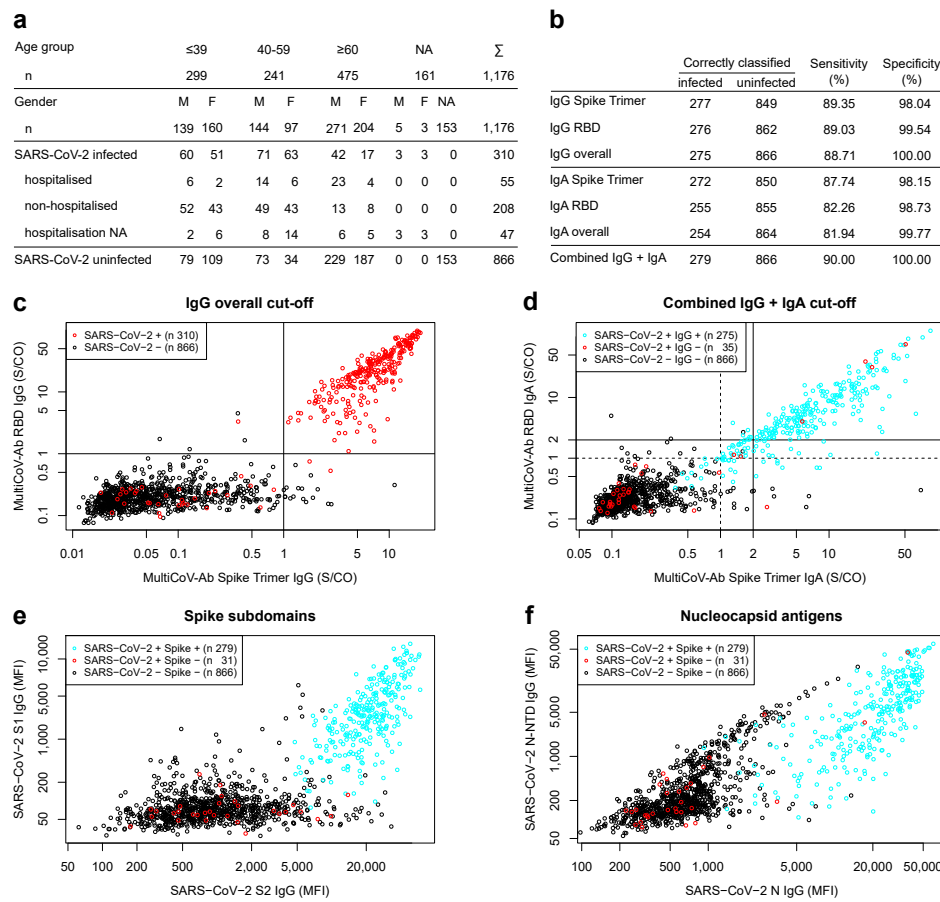


Figure 3

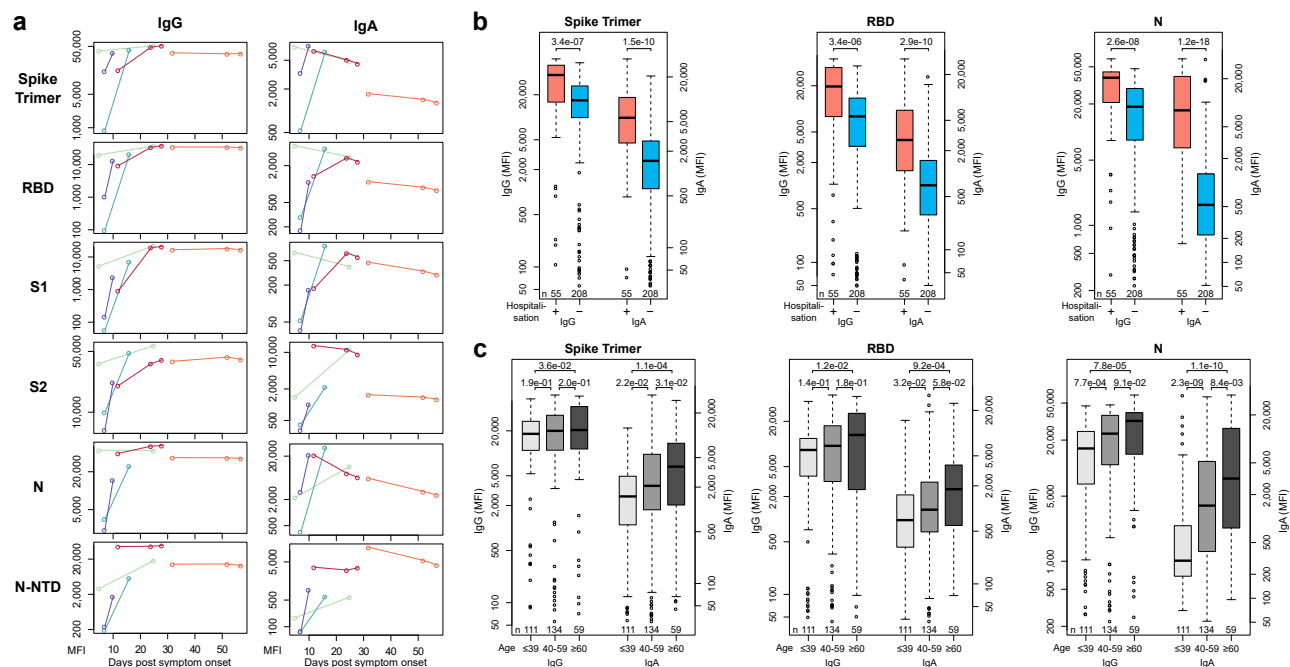
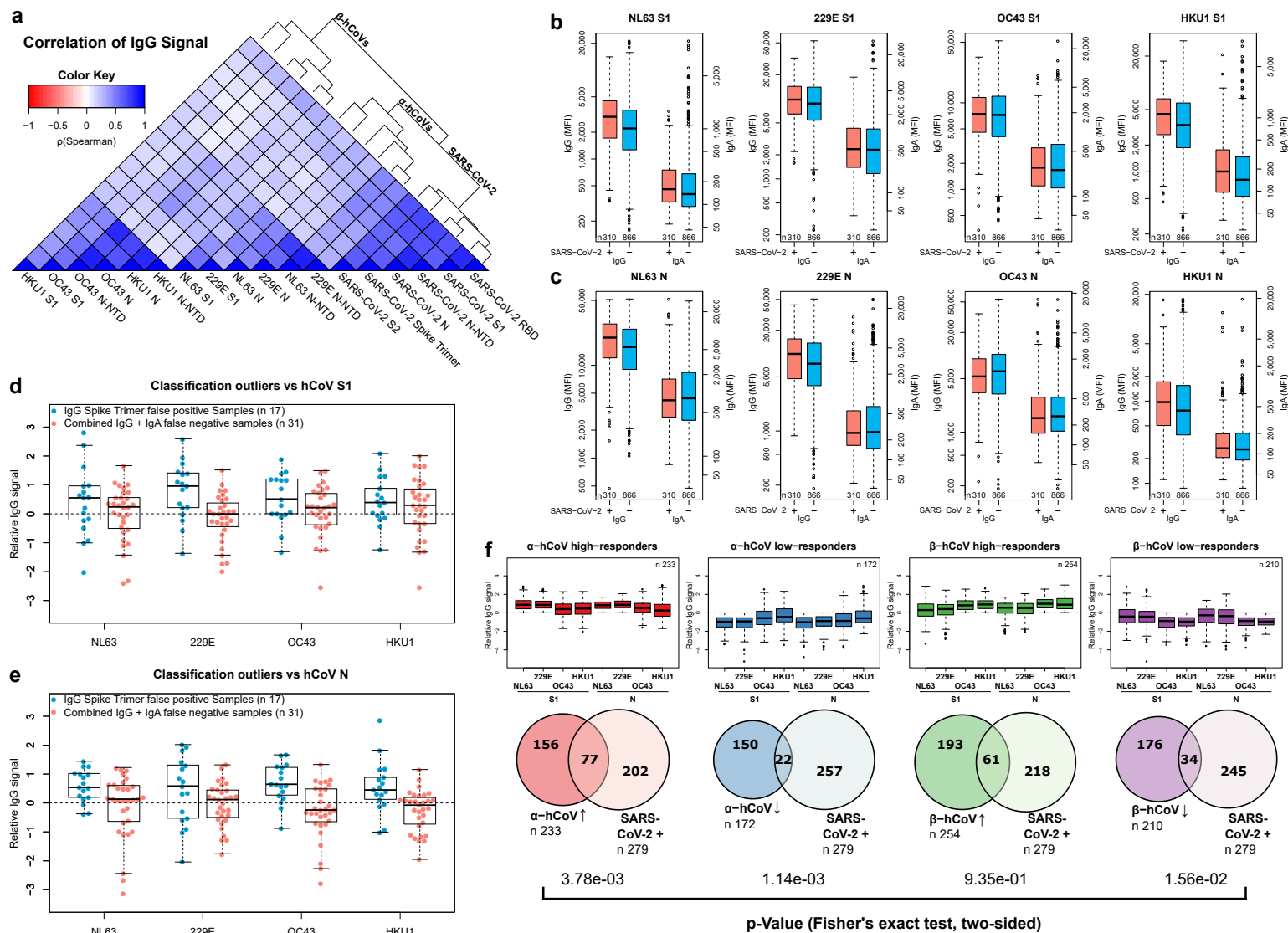


Figure 4



Extended Data - Table 1

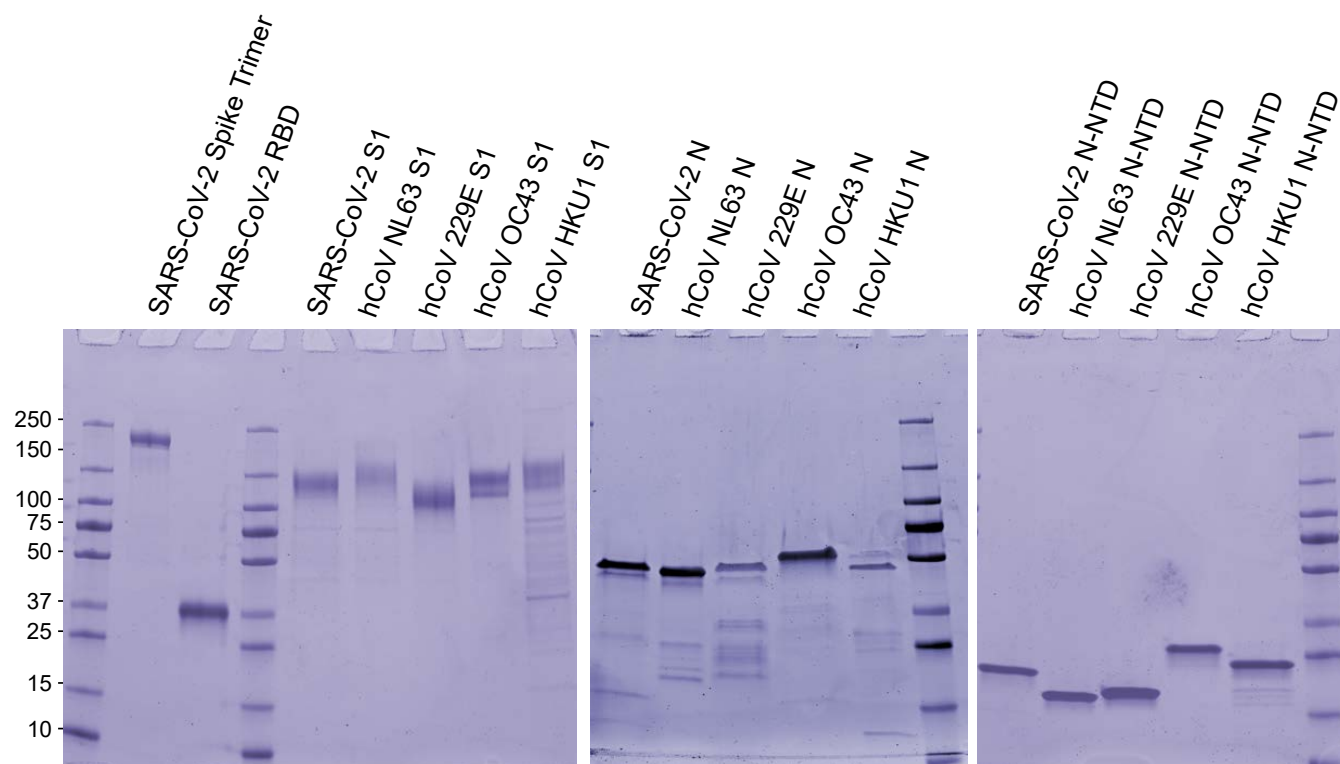
			SARS-CoV-2						hCoV NL63			hCoV 229E			hCoV OC43			hCoV HKU1		
			Spike																	
			Trimer	RBD	S1	S2	N	N-NTD	S1	N	N-NTD	S1	N	N-NTD	S1	N	N-NTD	S1	N	N-NTD
Inter-assay variance (%CV) n = 34, duplicates, 17 plates	IgG	QC1	3.7	3.3	3.4	3.7	2.8	7.4	3.5	3.2	4.4	3.3	2.8	5.2	3.1	6.0	4.4	3.4	4.7	5.4
		QC2	4.1	4.6	6.9	3.4	5.3	4.8	3.0	2.2	6.3	2.4	2.1	6.7	2.7	4.5	2.3	2.7	5.1	2.8
		QC3	3.4	2.4	2.3	3.6	2.1	4.6	3.1	2.5	3.5	2.9	2.0	4.7	2.9	6.4	4.6	3.2	3.2	3.5
		Blank	5.4	5.6	6.7	6.4	5.6	6.1	6.3	7.1	5.7	9.1	6.1	6.1	5.6	7.3	4.1	4.9	6.1	8.3
	IgA	QC1	3.9	4.6	4.9	4.0	5.1	5.0	4.2	3.6	3.9	4.0	5.3	7.4	4.3	7.4	5.0	4.2	6.0	5.0
		QC2	4.6	5.0	5.1	3.9	3.9	4.2	3.7	2.4	7.6	2.9	2.2	6.0	4.1	16.4	4.2	4.3	5.5	3.9
		QC3	3.9	3.8	4.5	3.4	3.4	4.8	3.9	2.8	4.0	3.0	5.1	4.5	3.6	6.1	4.1	3.7	4.5	5.1
		Blank	6.7	5.3	8.2	6.3	5.3	5.3	3.3	5.0	5.0	6.7	7.0	6.1	5.3	7.1	4.7	6.0	6.8	6.3
Intra-assay variance (%CV) n = 24	IgG	QC1	2.5	1.9	2.0	2.1	1.8	2.1	2.4	1.7	2.8	2.0	2.7	3.2	1.9	2.0	2.2	2.7	2.4	2.2
		QC2	5.9	4.3	4.1	2.8	2.7	3.2	1.9	1.9	2.6	2.0	2.2	2.7	2.2	1.6	2.1	2.5	3.1	2.5
		QC3	1.6	4.3	5.1	1.9	1.9	4.5	4.2	1.7	3.2	3.3	4.1	5.7	3.2	3.1	5.5	5.6	6.0	8.4
		Blank	6.0	5.6	5.2	5.8	5.2	4.2	5.0	4.8	4.8	7.3	6.2	6.3	6.5	6.2	4.4	6.1	6.0	6.2
	IgA	QC1	2.5	3.3	5.2	3.8	3.7	4.2	3.2	2.3	2.2	2.0	4.8	4.7	2.9	4.7	3.4	3.3	4.5	4.3
		QC2	4.8	5.7	5.7	3.2	4.1	4.3	3.4	2.0	5.7	2.1	2.1	6.1	3.0	3.1	1.9	3.9	6.4	3.8
		QC3	3.1	4.7	5.5	3.0	4.1	4.4	3.7	2.7	3.7	2.7	5.4	5.8	2.6	4.1	3.1	2.4	4.5	4.3
		Blank	5.8	5.3	6.3	5.0	5.4	5.5	4.5	5.6	5.3	7.2	6.3	7.0	6.7	9.5	7.3	5.2	8.8	7.0
LOD* (MFI) n = 24	IgG		32	26	23	29	38	33	29	28	26	65	35	24	33	30	33	37	33	25
	IgA		31	26	26	27	37	32	57	28	40	28	36	22	35	28	32	33	39	28

*Blank mean MFI + 3 * sd

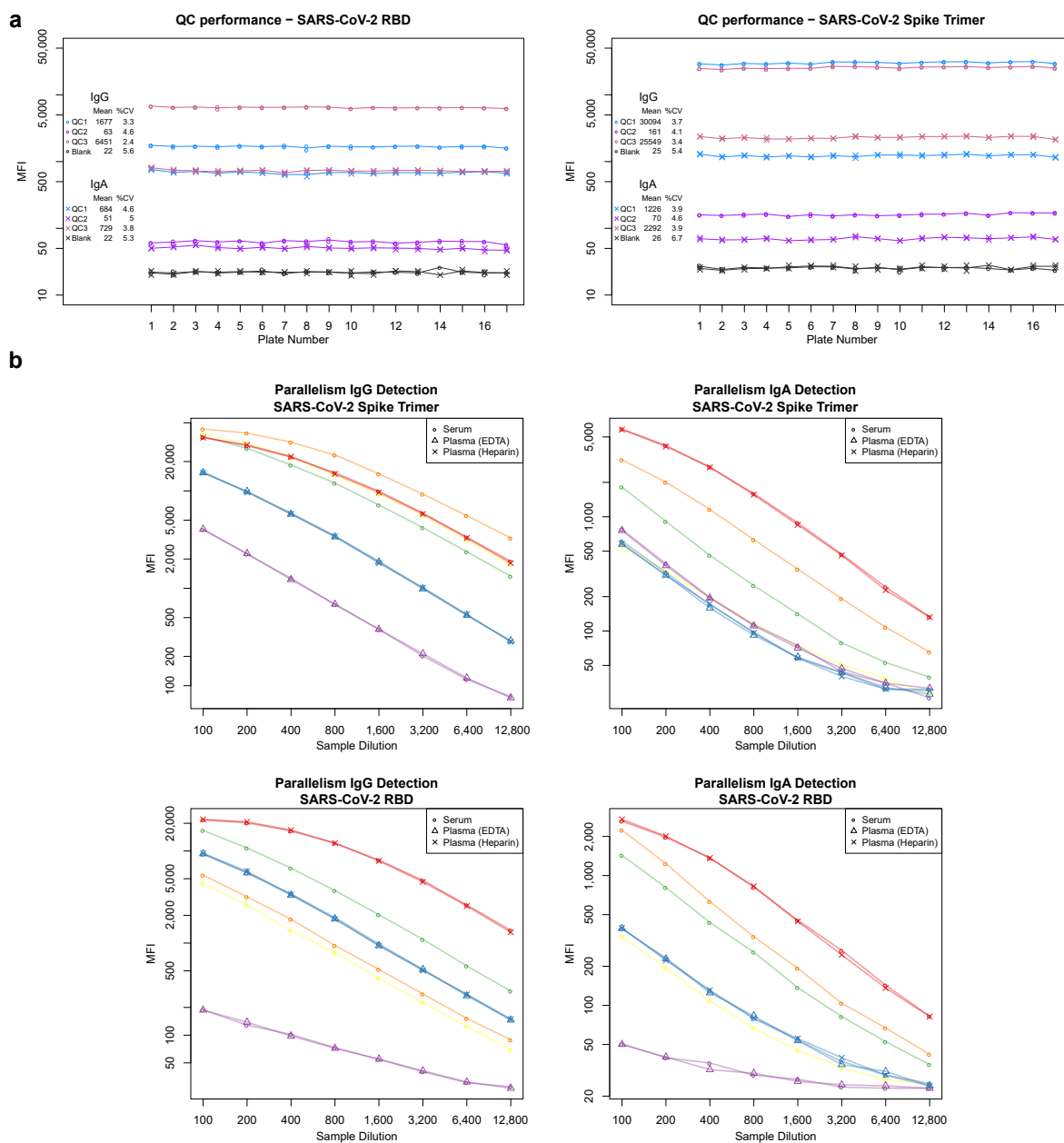
Extended Data - Table 2

Age n	≤39		40-59		≥60		NA			Σ
	299		241		475		161			1,176
Gender n	M	F	M	F	M	F	M	F	NA*	1,176
	139	160	144	97	271	204	5	3	153	
SARS-CoV-2-infected (total)	60	51	71	63	42	17	3	3	0	310
Hospitalized (for COVID19)	6	2	14	6	23	4	0	0	0	55
Non-Hospitalized	52	43	49	43	13	8	0	0	0	208
Hospitalisation NA	2	6	8	14	6	5	3	3	0	47
Patients with time series	2	0	0	0	2	1	0	0	0	5
SARS-CoV-2-uninfected (total)	79	109	73	34	229	187	2	0	153	866
Sample during pandemic	10	10	12	14	7	5	1	0	6	65
Sample pre-pandemic	69	99	61	20	222	182	1	0	147	801
Previous hCoV Infection	19	18	45	20	29	16	0	0	0	147
<i>confirmed NL63</i>	2	0	3	1	2	2	0	0	0	10
<i>confirmed 229</i>	5	1	4	1	5	4	0	0	0	20
<i>confirmed OC43</i>	0	1	14	1	6	5	0	0	0	27
<i>confirmed HKU1</i>	3	1	4	2	5	0	0	0	0	15
<i>unknown hCoV</i>	9	15	20	15	11	5	0	0	0	75
Pregnant	0	9	0	1	0	0	0	0	0	10
RF/HAMA samples	0	0	0	0	0	0	0	0	6	6
PCT > 3 ng/mL	0	0	0	0	0	0	0	0	21	21
Neuroinflammatory disease	6	6	1	0	1	1	0	0	0	15

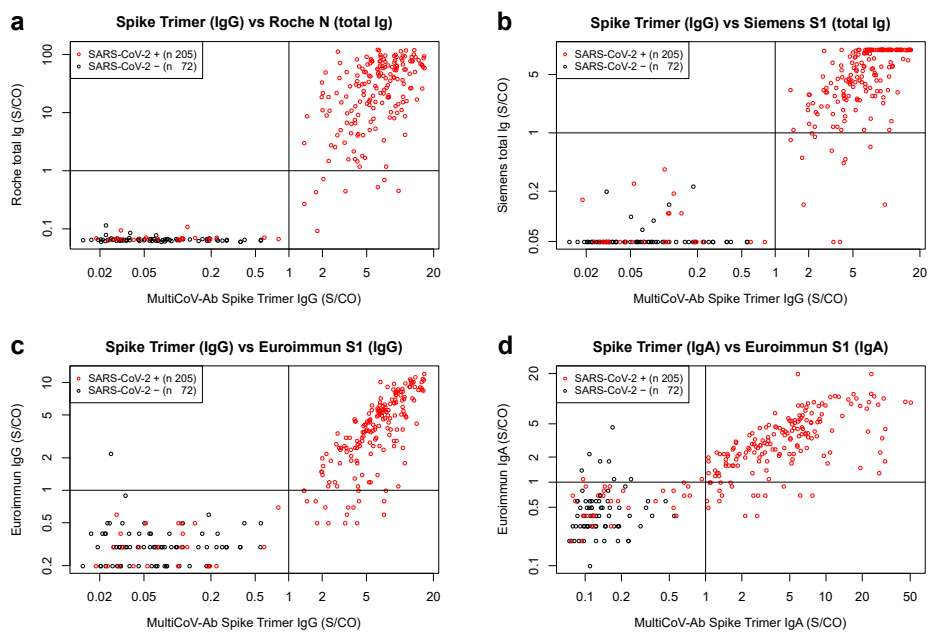
Extended Data - Figure 1



Extended Data - Figure 2



Extended Data - Figure 3



Extended Data Figure 4

